Transient Compressible Method of Exact Solutions Verification Problems: Two Fluid Systems Mechanically Coupled Through a Wall

Dan Hughes
March 2011

Abstract

The analysis given in these previous notes:

http://models-methods-software.com/2011/01/19/implicit-function-theory-applications-part-1-method-of-exact-solutions/

http://models-methods-software.com/2011/02/26/implicit-function-theory-single-fluid-system-calculations/

http://models-methods-software.com/2011/01/14/implicit-function-theory-applications-part-0/

are expanded to include the case of coupled fluid systems. Numerical solution results are given for an illustrative application.

The mathematical model, an exact continuous analogue of the discrete approximations used in many numerical solution methods, provides analytical and numerical-benchmark problems for verification by the Method of Exact Solutions (MES).

Introduction

A picture of the physical situation is shown in the nearby Figure 1. The coupling of the fluid systems is by means of deformable / flexible walls between the systems. As in the previous notes the mechanical case, coupling by pressure forces acting on the wall, is considered. The thermal case will be considered in future notes.

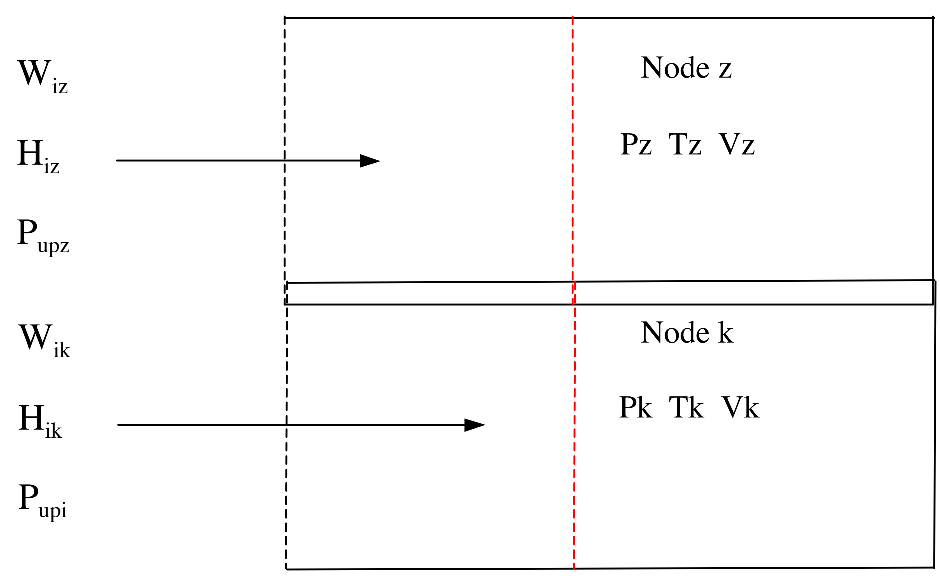

Figure 1. Geometry of the application.

Much of the details are available in the previous notes and will not be repeated here. The key to the approach is the use of implicit function theory to get the necessary derivatives of intensive thermodynamic state properties with respect to macroscopic extensive properties. These derivatives are reduced to expressions that contain thermodynamic state and thermo-physical material properties. Those derivatives for the mechanically-coupled case were given in Table 5 of previous notes here:

http://models-methods-software.com/2011/01/14/implicit-function-theory-applications-part-0/

That Table has some bugs in it which I have corrected and the corrected Table is shown here.

∂ of	with respect to	
	M_K	**E_K**
P_K	$\frac{1}{D}\left(1-\frac{h_k\beta_k}{C_{pk}}\right)V_k\left\{\frac{V_z^2}{C_{sz}^2}+K_wM_z\left(1-P_z\frac{\upsilon_z\beta_z}{C_{pz}}\right)\right\}$	$\frac{1}{D}\left(M_k\frac{\beta_k\upsilon_k}{C_{pk}}\right)\left[\frac{V_z^2}{C_{sz}^2}+K_wM_z\left(1-P_z\frac{\beta_z\upsilon_z}{C_{pz}}\right)\right]$
	M_Z	**E_Z**
	$\frac{1}{D}K_wM_kV_z\left(1-\frac{h_z\beta_z}{C_{pz}}\right)\left(1-P_k\frac{\beta_k\upsilon_k}{C_{pk}}\right)$	$\frac{1}{D}\left(K_wM_kM_z\frac{\beta_z\upsilon_z}{C_{pz}}\right)\left(1-P_k\frac{\beta_k\upsilon_k}{C_{pk}}\right)$
	M_K	**E_K**
P_Z	$\frac{1}{D}K_wM_zV_k\left(1-\frac{h_k\beta_k}{C_{pk}}\right)\left(1-P_z\frac{\beta_z\upsilon_z}{C_{pz}}\right)$	$\frac{1}{D}\left(K_wM_kM_z\frac{\beta_k\upsilon_k}{C_{pk}}\right)\left(1-P_z\frac{\beta_z\upsilon_z}{C_{pz}}\right)$
	M_Z	**E_Z**
	$\frac{1}{D}\left(1-\frac{h_z\beta_z}{C_{pz}}\right)V_z\left[\frac{V_k^2}{C_{sk}^2}+K_wM_k\left(1-P_k\frac{\upsilon_k\beta_k}{C_{pk}}\right)\right]$	$\frac{1}{D}\left(M_z\frac{\beta_z\upsilon_z}{C_{pz}}\right)\left[\frac{V_k^2}{C_{sk}^2}+K_wM_k\left(1-P_k\frac{\beta_k\upsilon_k}{C_{pk}}\right)\right]$
D	$\frac{V_k^2V_z^2}{C_{sk}^2C_{sz}^2}+K_w\left[M_z\frac{V_k^2}{C_{sk}^2}\left(1-P_z\frac{\beta_z\upsilon_z}{C_{pz}}\right)+M_k\frac{V_z^2}{C_{sz}^2}\left(1-P_k\frac{\beta_k\upsilon_k}{C_{pk}}\right)\right]$	

Table 5. Derivatives of equation of state properties with respect to mass and energy content for two flexible wall case.

The Effective Pressure-Wave Speed

The determinant of the Jacobian for the constraint functions is again in the last row of the Table. That expression can be written as

$$\left(\frac{V_k^2V_z^2}{C_{eff}^4}\right)=\frac{V_k^2V_z^2}{C_{sk}^2C_{sz}^2}+K_w\left[M_z\frac{V_k^2}{C_{sk}^2}\left(1-P_z\frac{\beta_z\upsilon_z}{C_{pz}}\right)+M_k\frac{V_z^2}{C_{sz}^2}\left(1-P_k\frac{\beta_k\upsilon_k}{C_{pk}}\right)\right] \quad (1.1)$$

Note that if the common wall between the nodes is rigid, $K_w = 0.0$, the following are obtained; (1) the derivatives of the pressure for either node with respect to the mass and energy content of the other node are zero see rows 2 and 3 of the Table, (2) that if the determinant for this case is substituted into the pressure derivatives with respect to the mass and energy content of the selected node these reduce to the results given in the previous table. For example,

$$\left(\frac{\partial}{\partial M_k}P_k\right)_{\ldots} = \frac{C_{sk}^2 C_{sz}^2}{V_k^2 V_z^2}\left(1-\frac{h_k\beta_k}{C_{pk}}\right)V_k\frac{V_z^2}{C_{sz}^2} = \frac{C_{sk}^2}{V_k}\left(1-\frac{h_k\beta_k}{C_{pk}}\right) \quad (1.2)$$

which is exactly what it should be and is the entry in the first row and first column of the first Table above. The same results will obtain for the remaining three derivatives.

The effective sound speed for the coupled fluid systems, from Eq. (1.1) is

$$C_{eff} = \sqrt[4]{V_k^2 V_z^2 / D} \quad (1.3)$$

The Equations

The equations for models of conservation of mass and energy content must be expanded to include these models for both nodes. To be explicit, and for convenient reference these are summarized in the following.

Mass conservation models for the nodes are

$$\frac{d}{dt}M_k = W_{ik}(t)$$

and (1.4)

$$\frac{d}{dt}M_z = W_{iz}(t)$$

where M is the mass of fluid in the pipe,

$$M = \rho V \quad (1.5)$$

and $W_i(t)$ is the mass flow rate of fluid into the pipe at the upstream boundary

$$W_i(t) = \rho_i U_i A_{fi} \quad (1.6)$$

where ρ is the fluid density, U is the fluid speed at the entrance of the pipe, and A_f is the flow area for the pipe. The initial condition is

$$M_i(0) = M_{0i} \quad (1.7)$$

Energy balance model equations, based on total internal energy content for the fluid, are

$$\frac{d}{dt}E_k = h_{ik}W_{ik}(t) - P_k\frac{d}{dt}V_k$$
and (1.8)
$$\frac{d}{dt}E_z = h_{iz}W_{iz}(t) - P_z\frac{d}{dt}V_z$$

where h_i is the enthalpy of the fluid entering the pipe at the upstream boundary and the energy content for the fluid is

$$E = Mu = \rho V u \tag{1.9}$$

where u is the specific internal energy for the fluid. The initial condition for the fluid energy content is

$$E(0) = E_0 \tag{1.10}$$

Neglecting all terms in a momentum balance model except for the pressure gradient, momentum equation models for the fluid flow into the pipes at the upstream end are

$$\frac{d}{dt}W_{ik} = \frac{A_{fk}}{L_{\Delta P}}\left(P_{upk} - P_k\right)$$
and (1.11)
$$\frac{d}{dt}W_{iz} = \frac{A_{fz}}{L_{\Delta P}}\left(P_{upz} - P_z\right)$$

where P_{up} is the constant upstream pressure and $L_{\Delta P}$ is a representative distance for the pressure gradient; one-half the total pipe length. The initial condition is

$$W_i(0) = W_i^0 \tag{1.12}$$

Note that wall friction and gravity have not been included. Gravity is easily included, because it's a constant term, but wall friction is not. For verification purposes, the wall friction can be minimized by use of a few different techniques available in most models and codes; make the pipe diameter be really big, for example.

The wall function for node '*k*' for the coupled-node case is

$$V_k = V_{k0} + K_w[\left(P_k(t) - P_k(0)\right) - \left(P_z(t) - P_z(0)\right)] \tag{1.13}$$

with a corresponding equation for node '*z*'.

For the case of two nodes coupled through a deformable wall, the EOS for the pressure for node '*k*' is,

$$P_k = \hat{P}_k(M_k, E_k, M_z, E_z) \tag{1.14}$$

with a similar expression for node '*z*'. Carrying out the procedure used for the single-node case gives the time derivative for the pressure

$$\begin{aligned}\frac{d}{dt}P_k = &\left(\frac{\partial}{\partial M_k}\hat{P}_k\right)_{\dots}\frac{d}{dt}M_k + \left(\frac{\partial}{\partial E_k}\hat{P}_k\right)_{\dots}\frac{d}{dt}E_k \\ &+\left(\frac{\partial}{\partial M_z}\hat{P}_k\right)_{\dots}\frac{d}{dt}M_z + \left(\frac{\partial}{\partial E_z}\hat{P}_k\right)_{\dots}\frac{d}{dt}E_z\end{aligned} \tag{1.15}$$

with a similar expression for node '*z*'.

Putting the appropriate mass and energy equations into the derivative of the pressure gives two equations for the pressure responses.

$$\begin{aligned}\frac{d}{dt}P_k = &\left[\left(\frac{\partial \hat{P}_k}{\partial M_k}\right)_{\dots} + h_{ik}\left(\frac{\partial \hat{P}_k}{\partial E_k}\right)_{\dots}\right]W_{ik}(t) \\ &+\left[\left(\frac{\partial \hat{P}_k}{\partial M_z}\right)_{\dots} + h_{iz}\left(\frac{\partial \hat{P}_k}{\partial E_z}\right)_{\dots}\right]W_{iz}(t)\end{aligned} \tag{1.16}$$

and

$$\begin{aligned}\frac{d}{dt}P_z = &\left[\left(\frac{\partial \hat{P}_z}{\partial M_k}\right)_{\dots} + h_{ik}\left(\frac{\partial \hat{P}_z}{\partial E_k}\right)_{\dots}\right]W_{ik}(t) \\ &+\left[\left(\frac{\partial \hat{P}_z}{\partial M_z}\right)_{\dots} + h_{iz}\left(\frac{\partial \hat{P}_z}{\partial E_z}\right)_{\dots}\right]W_{iz}(t)\end{aligned} \tag{1.17}$$

The pressure-volume work term, the last term on the right-hand side of Eqs. (1.8), has been omitted. The terms is easily handled by numerical methods, but is generally sufficiently small that it can be neglected.

Calculations

Inlet Flow Specified

If the mass flow rate into each node is specified as a function of time, such as

$$W_i = B_i - D_i t \tag{1.18}$$

all the model equations can be directly integrated. The results are straightforward and will not be summarized here. A spreadsheet can be used to get numerical values given the necessary thermodynamic state and thermophysical fluid properties and the derivatives summarized in the Table above.

Initial Flow and Pressure Specified

This more general case does not lead to straightforward analytical integration of the model equations. I have used a couple of numerical means to get some results. A simple Euler numerical method provides a way to get results without much programming effort. The bigger problem is getting all the material thermodynamic state and thermophysical properties and beyond that, ensuring that the equations given in Table 1 are correct. And then ensuring that all that has been correctly programmed.

Note that several different calculations can be obtained by specialization of the two-node case. Including rigid-wall results by assigning K_w to be zero, and one-node flexible-wall results by making one of the nodes sufficiently large that the fluid pressure remains constant in that node. A null case is obtained by setting geometry, ICs and BCs to be the same for each node. For all the cases considered in these notes, another test can be obtained by changing the finite difference gird in the problem specifications so that a change in the sign of the mass flow is obtained and all else is the same.

The solution for the case of an initial flow is specified and sudden stopping of that flow in either or both of the nodes requires numerical solution of the coupled equations for $P_k(t)$ and $P_z(t)$.

For this case we need to solve the momentum equation model, Eqs. (1.11), for the mass flow rate into the pipe inlet. These equations are coupled through the dependency of the pressure in each node on the state of the fluid in the adjacent node; Eqs. (1.16) and (1.17). This coupling must be sufficiently accounted for in the numerical solution method. The derivation will be carried out for the 'k' node in the following discussions.

A straightforward finite-difference approximation for the momentum-balance model for the node from the first of Eqs. (1.11) is

$$\left(\Delta W\right)_{ik}^{n+1} = \left(\Delta t\right)\frac{A_f}{\left(L/2\right)}\left(P_{upk} - P_k^{n+1}\right) \tag{1.19}$$

where the upstream pressure has been taken to be constant. If that pressure is a specified function of time, the function can be easily evaluated at the new-time level. A first-order Taylor-series expansion of the node pressure from Eq, (1.14) is

$$\begin{aligned} P_k^{n+1} = P_k^n &+ \left(\frac{\partial P_k}{\partial M_k}\right)_{\ldots}^n \left(\Delta M_k\right)^{n+1} + \left(\frac{\partial P_k}{\partial E_k}\right)_{\ldots}^n \left(\Delta E_k\right)^{n+1} \\ &+ \left(\frac{\partial P_k}{\partial M_z}\right)_{\ldots}^n \left(\Delta M_z\right)^{n+1} + \left(\frac{\partial P_k}{\partial E_z}\right)_{\ldots}^n \left(\Delta E_z\right)^{n+1} \end{aligned} \tag{1.20}$$

Discrete approximations for the mass and energy model equations, Eqs. (1.4) and (1.8) respectively, for the '*k*' node are

$$\left(\Delta M_k\right)^{n+1} = \left(\Delta t\right)W_{ik}^n + \left(\Delta t\right)\left(\Delta W\right)_{ik}^{n+1} \tag{1.21}$$

and

$$\left(\Delta E_k\right)^{n+1} = \left(\Delta t\right)h_{ik}W_{ik}^n + \left(\Delta t\right)h_{ik}\left(\Delta W\right)_{ik}^{n+1} \tag{1.22}$$

where the pressure-volume work term has been omitted for convenience in the word processing.

Putting the discrete mass and energy model equations into Eq. (1.20), omitting the pressure-volume work terms from the energy-content model of Eqs. (1.8) in the typing, but carrying it at the old-time level in the coding, and using the results in the Table above gives

$$\begin{aligned} P_k^{n+1} = P_k^n &+ \frac{V_k}{D}\left[\frac{V_z^2}{C_{sz}^2} + K_w M_z V_k\right]\left[\left(\Delta t\right)W_{ik}^n + \left(\Delta t\right)\left(\Delta W\right)_{ik}^{n+1}\right] \\ &+ \frac{1}{D}K_w M_k V_z\left[1 - P_k\frac{\beta_k \upsilon_k}{C_{pk}}\right]\left[\left(\Delta t\right)W_{iz}^n + \left(\Delta t\right)\left(\Delta W\right)_{iz}^{n+1}\right] \end{aligned} \tag{1.23}$$

with a corresponding similar equation for the pressure for node '*z*'.

Putting this into Eq. (1.19) gives an equation for the change in the mass flow rate at the inlet to the fluid system. The second equation for the two dependent variables in these equations is obtained by use of the momentum-balance model for the '*z*' node.

Those two equations can be analytically solved for the change in the mass flow rate and those solutions coded in the numerical solution method for all the other equations.

I have not yet carried out this program. Instead the explicit, fourth-order Runga-Kutta method was used to solve the equations.

Calculated Results

For an initial verification-like calculation, the initial mass flow rate at the inlet to the nodes was set to 0.0 and the upstream pressure set to the initial value in the nodes. This null transient should result in no changes in any of the dependent variables for all times.

For a second verification calculation, the ICs and BCs for the coupled nodes are identical and mechanical coupling between the nodes is negated by setting $K_w = 0.0$. The expected results include; (1) the volume of the nodes should not change, (2) the response of all dependent variables for both nodes should be exactly the same, and (3) the numerical results should correspond to those for the case of a single node having the same ICs and BCs.

A third calculation with ICs and BCs equal for the nodes and $K_w \neq 0.0$ should show that (1) and (2) are still obtained, but (3) is not obtained because the effective pressure-wave speed does not correspond to the value for a single isolated node.

A final verification calculation set the volume of one of the nodes to an enormous value so that the pressure in that node would be constant. Additionally, as shown by Eq. (1.11), under this condition the right-hand-side of the momentum equation model is constant and the mass flow rate into the node will increase linearly with time.

All the verification calculations proved to be successful.

The following calculations used the same dimensions and properties for the nodes as were used in the previous notes. The node dimensions are summarized in the nearby Table 1 and the node-material properties are given in the following Table 2.

Dimension	**Value**
Length (m)	10.00
Flow Area (m^2)	1.00
Diameter (m)	1.1284
Wall Thickness (m)	0.00635

Table 1. Dimensions of the pipe and pipe wall.

Property	Value
Density	7600.0 to 8200.0
Thermal Expansion Coefficient (m/m K)	1.7×10^{-5}
Bulk Modulus $\left(N/m^2\right)$	1.66×10^{11}
Shear Modulus $\left(N/m^2\right)$	7.7×10^{10}
Tensile Modulus $\left(N/m^2\right)$	1.16×10^{11}
Young's Modulus $\left(N/m^2\right)$	2.07×10^{11}
Poisson's Ratio	0.30
K_{wall} (m^5/N)	7.8118×10^{-9}
Table 2. Material properties for stainless steel.	

The fluid properties are summarized in the nearby Table 3.

Property	Value
P (MPa)	0.20
T (K)	350.0
ρ (kg/m^3)	973.797
C_p (J/kg K)	4191.25
C_v (J/kg K)	3887.84
β (1/K)	6.2226×10^{-4}
κ (m^2/N)	4.5869×10^{-10}
u (J/kg)	3.2163×10^{5}
h (J/kg)	3.21841×10^{5}
$\left(\frac{\partial P}{\partial \rho}\right)_T$ (J/kg)	2.23878×10^{6}
$\left(\frac{\partial P}{\partial T}\right)_\rho$ (N/m^2K)	1.3566×10^{6}
C_{sf} (m/s)	1553.54
Table 3. Water properties.	

Results from an illustrative calculation with unequal ICs and BCs are summarized in the following discussions. The initial node pressure and temperature were 0.20 MPa and 350.0 K, respectively. A calculation using the RK4 method and with the upstream pressure constant at $2.8x10^5$ Pa for each node and with a flexible wall gives the following results. For the conditions summarized in the Tables, the effective pressure-wave speed is about 1197.2 m/s. The initial mass flow rate was set to 6.0 kg/s for node '*k*' and 12.0 kg/s for node '*z*'.

The pressure response for the two nodes is shown in Figure 2.

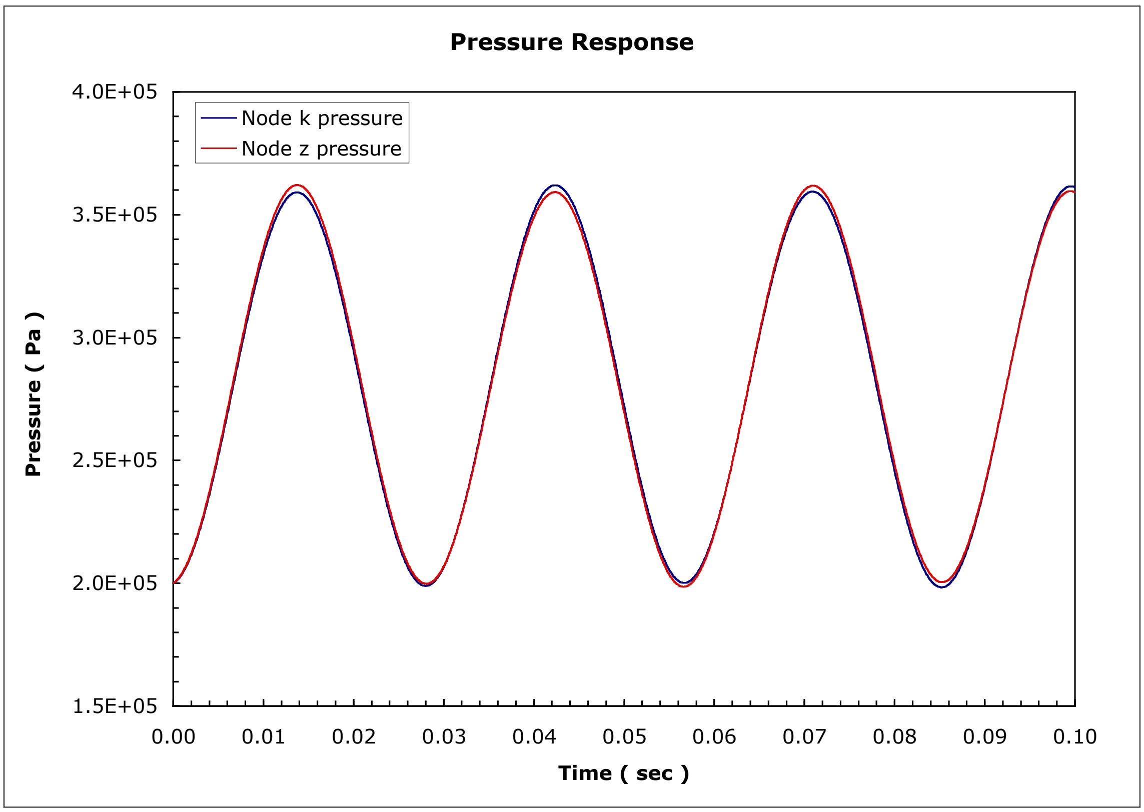

Figure 2. Pressure response for the nodes as a function of time.

The pressure difference between the nodes doesn't show too god, so that is given in Figure 3.

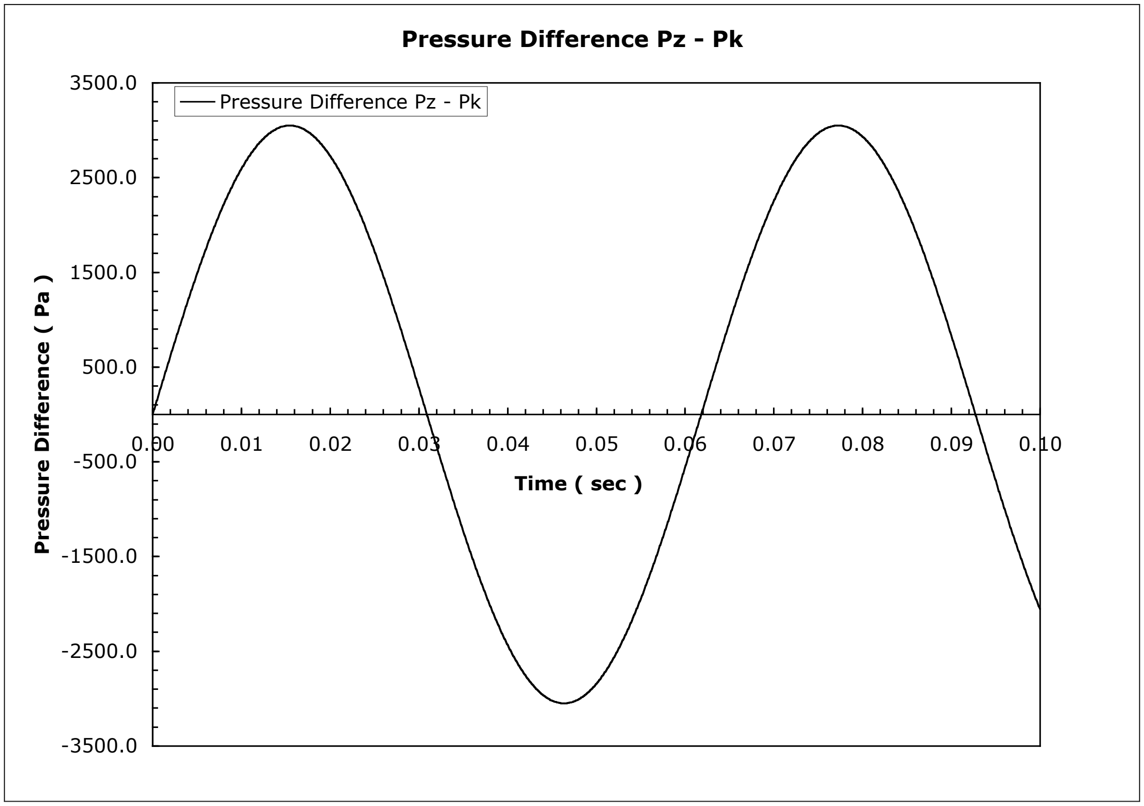

Figure 3. Pressure difference between the nodes as a function of time.

The response of the change in the volume for node 'z' is shown in Figure 4.

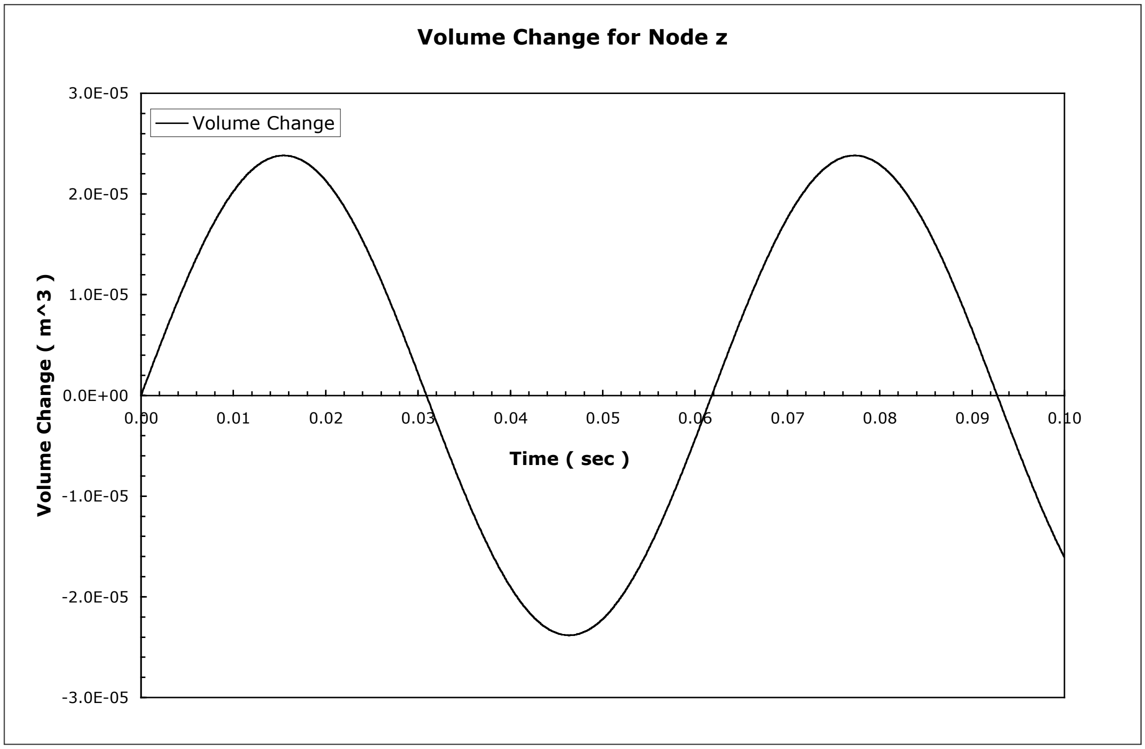

Figure 4. Change in the volume for node 'z'.

The mass flow rate response at the node inlet is shown in Figure 5.

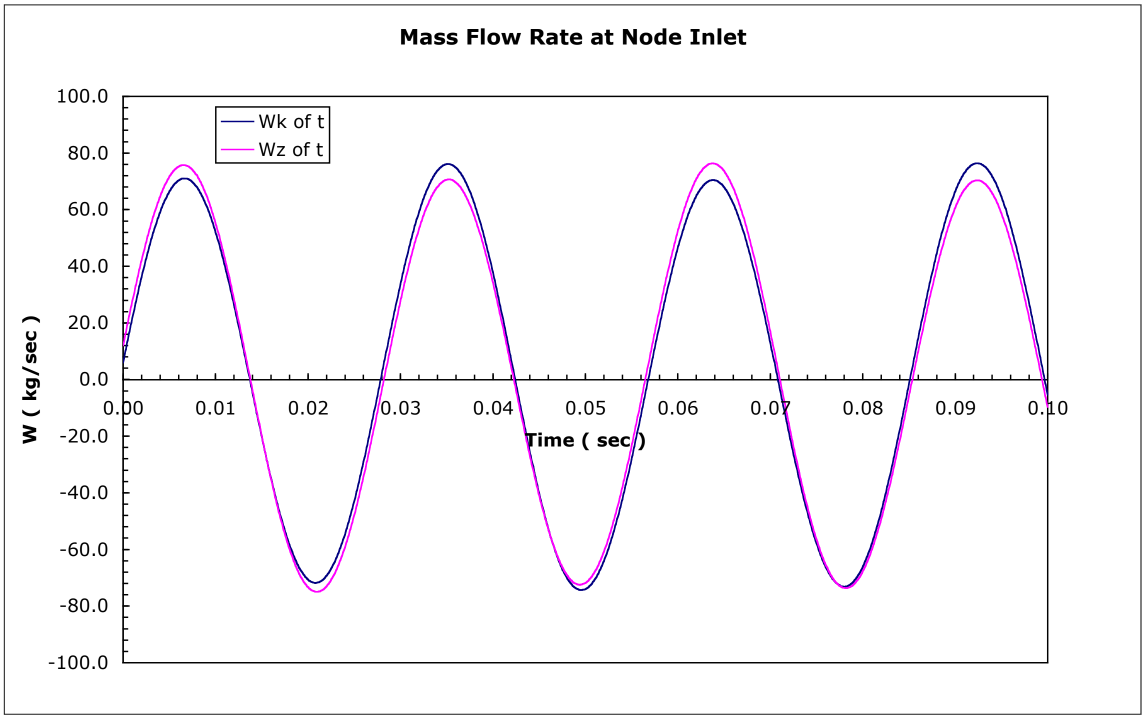

Figure 5. Pressure difference between the nodes as a function of time.

Conclusions

These problems offer several verification opportunities as Method of Exact Solutions (MES) problems for transient, compressible flows both with and without fluid-structure interactions.

Several numerical-benchmark-grade verification problems can be devised and the ODEs solved by off-the-shelf solver software used to present the expected results. I plan to pursue this aspect if the proposed paper is accepted for publication.